Active Sonar-Driven Iceberg Wall Following Path Planner for Autonomous Underwater Vehicles

Tony Jacob

Department of Ocean Engineering

University of Rhode Island

tony.jacob@uri.edu

Mingxi Zhou

Graduate School of Oceanography
University of Rhode Island
mzhou@uri.edu

Abstract—Autonomous Underwater Vehicles (AUV) are potential candidates for mapping icebergs in a safer manner compared to using manned ships. However, iceberg drifts and irregular contour pose challenges for AUVs when maneuvering around the iceberg at a constant stand off distance autonomously. To this end, in this paper, we present a novel approach for generating guidance path for an AUV based on an Occupancy Grid Map (OGM) constructed from the measurements from a Mechanical Scanning Imaging Sonar (MSIS). The method consists of three components: MSIS data pre-processing, path generation and waypoint selection, to realize the autonomous iceberg wallfollowing behaviour. The presented method is generalized and can be utilized for other online wall following applications. The autonomy system is validated in a simulation environment where the AUV has successfully circumnavigated different icebergs at desired standoff distance of 20 meters and has produced an overall root-mean-square-error less than 4m.

Index Terms—Autonomous Underwater Vehicles (AUVs), Path Planning, Iceberg Mapping, Mechanical Scanning Imaging Sonar (MSIS), Occupancy Grid Maps (OGM)

I. INTRODUCTION

Icebergs, broken away from polar glaciers and ice shelves, drift in the ocean towards low latitude regions. They disrupt marine transportation, and affect ocean currents and climate by inducing cold freshwater plumes [1]. To better quantify their impacts, icebergs, especially the underwater portion (about 88-90% of the overall shape), has to be measured. Recent studies have found that Autonomous Underwater Vehicles (AUVs) can be potential candidates for iceberg mapping [2] and [3]). However, advanced autonomy is needed for obstacle avoidance, online path planning and relative navigation algorithms for a safe and successful AUV-based iceberg mapping mission [4]. Particularly, the autonomy should account for the irregular contour of the iceberg such that the AUV can be maintained at a desired standoff distance for consistent sensing footprints and measurement resolution, resulting in reliable mapping data products.

In this paper, we present a new autonomy system for AUV-based iceberg circumnavigation using a MSIS. The method has three major components. In Section II.A, we first present a new data processing pipeline and an adaptive filtering technique to extract valid obstacle MSIS returns for creating occupancy grid

This work is supported by the National Science Foundation (NSF) under the award #2221676, and the Graduate School of Oceanography, University of Rhode Island.

maps (OGM). We have tested the MSIS processing pipeline both in tank and simulation environments. Secondly, in Section II.B, we present an image-based approach for generating a guidance path for AUVs from the OGM. The path is generated based on the extracted local iceberg contour such that the AUV can be maintained at a specific standoff distance. In order to successfully parameterize the local contour into a polynomial equation, we introduce the concept of creating a temporal frame that is defined based on the local iceberg contour. The orientation of this frame is adapted to alleviate the potential problem of having invalid solutions when parameterizing the contour into a polynomial equation. Third, in Section II.C, we introduce a heuristic that selects the waypoint from the derived path which then is given to the vehicle guidance system to follow. The online path planner has been successfully validated in Stonefish [5] with the ALPHA AUV [6] and drifting icebergs with results shown in Section III.

II. METHODOLOGY

A. MSIS Preprocessing and Costmap Generation

The MSIS is placed under the nose of the AUV. Since the vehicle is restricted to clockwise circumnavigation, we programmed the sonar to scan within a sector from 30° on the vehicle's port side to 135° on the vehicle starboard side. This geometry allows for sufficient coverage of the iceberg (ahead and behind of the vehicle) with the scan time of 13s while the vehicle is in motion. The maximum range of the MSIS is 50 m and the stepping angle is configured at 0.9°.

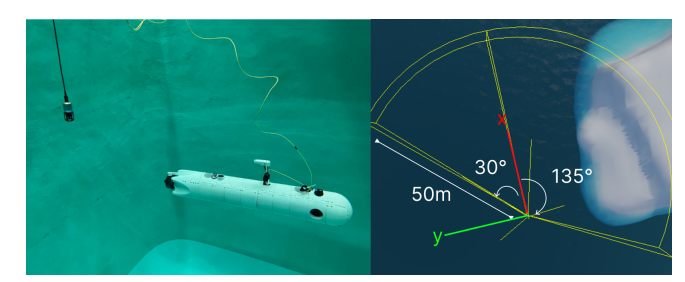


Fig. 1. Left: ALPHA AUV in tank. Right: ALPHA AUV and Iceberg in the Stonefish Environment.

In pre-processing, the measurements from MSIS are first converted into a point cloud based on the echo intensity over the range, the current scanning angle, the corresponding vehicle pose, the relative orientation and location from the sonar to the vehicle's body frame. Second, for each ping, we eliminate the points with echo intensities received within 2 meters from the sensor to remove the ringing effects. Next, an adaptive filter is implemented to remove the points with return intensities less than a threshold as defined in Eq. 1 where μ and σ are the mean and standard deviation of the intensities of the points and k is a user-defined parameter which was set to 2 in our case.

$$I_{\text{threshold}} = \mu + k\sigma$$
 (1)

The resultant point clouds are then projected into a 2D local vehicle-fixed frame and are used to update the OGM, whose width and length are equal to the sonar range. In each cell of the OGM, an intensity value is assigned to indicate the probability of existence of an obstacle based on incremental measurements ([7] and [8]).

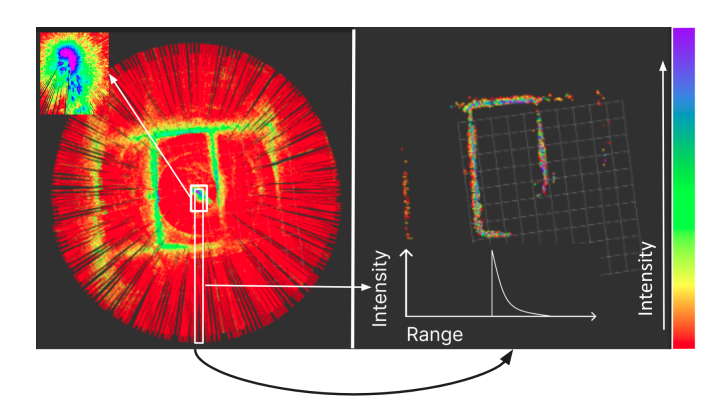


Fig. 2. Left: PointCloud2 representation of data from BlueRobotics Ping360 measurements from an indoor water tank. Zoom-in figure in the left: The high intensity measurements near the sensor due to ringing effects. Right: Result of the statistical filtering $\mu+2\sigma$ and radial distance filtering. Some returns from the multipath still exist after filtering.

B. Path Generation

To extract the iceberg contour and generate the desired AUV path, we treat the OGM as an image (Figure 3A) and apply the following imaging processing algorithms. First, the OGM image is dilated to fill the internal voids (Figure 3B). Second, the Canny Edge [9] detector is applied to extract the edges in the image (Figure 3C). Third, for each azimuth angle (0.1 rad) from the center of the image (the AUV), we extract the cells with the shortest range to the center, which forms the local contour of the iceberg (Figure 3D).

After the local iceberg contour have been extracted from the OGM, a series of reference frames (Figure 4) are created for generating a collision-free path. First, from the *Image Frame*, {I} of the vehicle-relative OGM, the point with the lowest y-coordinate value is defined to be the origin of a new reference frame, named *Edge Frame* {E}, where all other points are transformed to. Second, we define a local iceberg contour coordinate frame, named *Line Frame* {L} based on the trend of the points in {E} frame.

Since the general line equation does not handle vertical lines, the trend of the points is determined using Eq 2 to 5 as presented in [10].

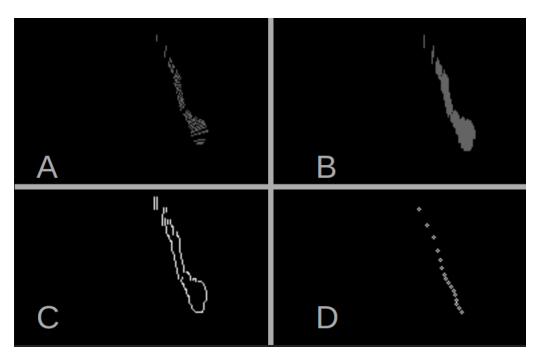


Fig. 3. A: The raw image from the OGM. B: The resulting image after dilation. C: After applying Canny Edge algorithm. D: The final estimation of the iceberg surface contour in the processed image.

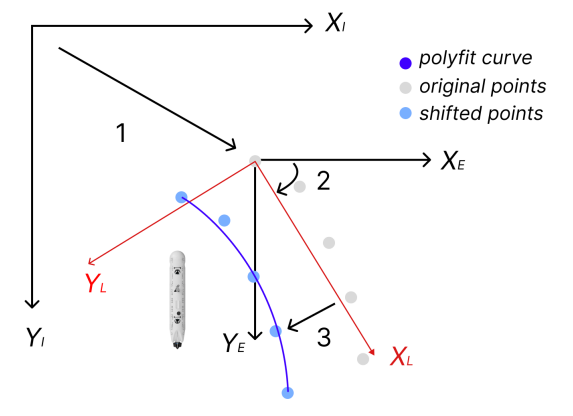


Fig. 4. The series of transformations between coordinate frames to generate waypoints that are at a constant stand off distance and analogous to the local iceberg contour. (1): Transformation from $\{I\}$ to $\{E\}$. (2): Creating $\{L\}$ based on the local trend of the contour. (3): Applying the constant stand off distance. The new series of points are transformed back to $\{E\}$ and then $\{I\}$.

$$S_{XX} = \sum_{i=1}^{J} (x_i - \bar{x})^2$$
 (2)

$$S_{YY} = \sum_{i=1}^{j} (y_i - \bar{y})^2 \tag{3}$$

$$S_{XY} = \sum_{i=1}^{j} (x_i - \bar{x})(y_i - \bar{y})$$
 (4)

$$\beta_1 = \begin{cases} \frac{S_{XY}}{S_{XX}}, & \text{if} \quad S_{XX} \ge S_{YY} \\ \frac{S_{YY}}{S_{XY}}, & \text{otherwise} \end{cases}$$
 (5)

We compute the sum of squared deviations from the mean value of X (Eq. 2) and sum of squared deviations from the mean value of Y (Eq. 3) where \bar{x} and \bar{y} represent average values of x and y coordinates, respectively. The sum of the product of the differences between x values and \bar{x} as well as the differences between y values and \bar{y} is also calculated in Eq. 4. Given the general line equation, $y = \beta_0 + \beta_1 x$, we find

the least squares estimates of β_1 as stated in [11] where S_{XY} is divided by the S_{XX} or S_{YY} based on the condition shown in Eq. 5. In the second case, β_1 is with respect to X of the general line equation. In such cases, β_1 is then transformed with respect to Y by taking its inverse. After we have obtained the slope, β_1 , the iceberg surface points are then transformed into $\{L\}$. The vehicle coordinate (center of the OGM) is also transformed into $\{L\}$.

Next, the contour is shifted in $\{L\}$ with the desired standoff distance. As shown in Figure 5, if the y-coordinate of the vehicle in the $\{L\}$ frame is positive, the contour is shifted by increasing the y-coordinate values and vice versa. This ensures that the contour is moving towards the vehicle regardless of the trend of the line and vehicle pose.

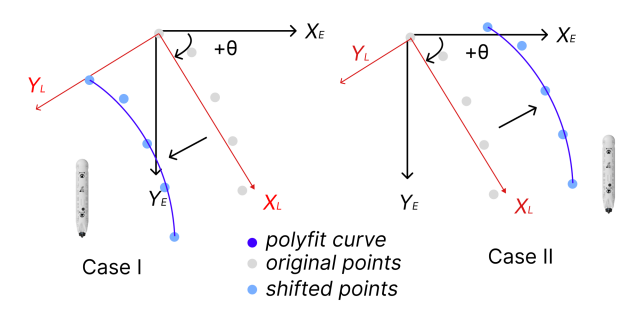


Fig. 5. The path is shifted towards the vehicle in {L}. Left: If the vehicle's y-coordinate in {L} is positive, the contour is shifted by increasing the y-coordinate values. Right: vice versa.

Finally, the shifted contour is parameterized into a polynomial equation, $y = ax^2 + bx + c$, that allows for an accurate representation of the actual iceberg shape instead of a linear approximation as in the previous works [4] and [10]. Once the coefficients of the polynomial function are found, we generate a series of points characterising the respective polynomial in the $\{L\}$ frame. Compared to the existing works in rugged seafloor following planners [12], this method does not require the 2.5D terrain assumption making this a more general solution.

C. Path Following

Our path following methodology has two modes - *Following* and *Iceberg Reacquisition* depending on whether or not there is enough sonar coverage of the iceberg to generate a path.

$$d_{V,i}^{L} = \sqrt{(X_i^L - X_V^L)^2 + (Y_i^L - Y_V^L)^2}$$
 (6)

$$\psi_{V,i}^{L} = \begin{cases} atan2(\frac{Y_{i}^{L} - Y_{V}^{L}}{X_{i}^{L} - X_{V}^{L}}) - \pi, & \text{if} \quad Y_{V}^{L} > 0\\ atan2(\frac{Y_{i}^{L} - Y_{V}^{L}}{X_{i}^{L} - X_{V}^{L}}), & \text{otherwise} \end{cases}$$
(7)

$$\psi_{i,i+1}^{L} = atan2\left(\frac{Y_{i+1}^{L} - Y_{i}^{L}}{X_{i+1}^{L} - X_{i}^{L}}\right)$$
 (8)

$$Cost = \left[\frac{d_{V,i}^{L}}{u} + \left| \frac{(\psi_{V,i}^{L} - \psi_{i,i+1}^{L})}{r} \right| \right]$$
 (9)

1) Following Mode: For an effective clockwise circumnavigation of the iceberg and always ensuring forward course, the selection of the waypoint for pure pursuit guidance [13] is calculated in {L}. First, we compute the metrics to determine the cost for each point on the generated path.. The distance of the points from the vehicle in {L} frame is calculated using Eq. 6. Depending on how the path was shifted (Fig. 5), the vehicle to point angle, ψ_i^L is calculated accordingly as shown in Eq. 7. If the path is shifted towards positive Y of $\{L\}$ frame, then the angle is inverted by π radians. The track angle of each point are also calculated in {L} frame as shown in Eq. 8. Second, we compute the cost for each point based on the three metrics mentioned above. As shown in Eq. 9, the distance d is divided by the vehicle's maximum surge velocity (u) and the absolute difference of the angles $(\psi^L_{V,i}$ and $\psi^L_{i,i+1})$ are divided by the vehicle's maximum yaw rate(r). These components are summed together for each valid point thereby converting them into a measure of time-to-intercept.

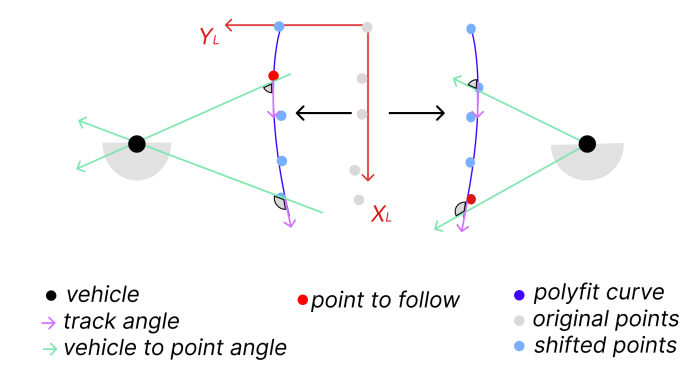


Fig. 6. Depending on how the path was shifted (Fig. 5), the vehicle to point angle is calculated accordingly. Left: If path is shifted towards positive Y of $\{L\}$ frame, then the angle is inverted by π radians. Right: if the path is shifted towards negative Y, then angle is calculated as is. The point with the lowest cost that falls in $(-\pi/2, \pi/2)$ of the line frame is then selected for pure pursuit guidance.

Finally, the point with the minimum cost that falls between $(-\pi/2, \pi/2)$ of the line frame is then converted back to world frame and then fed into the vehicle's guidance system [14]. This heuristic enables the vehicle to track the path and minimize cross track error while circumnavigating the iceberg in clockwise fashion.

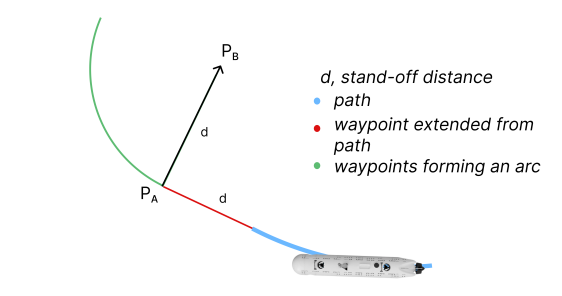


Fig. 7. In the absence of valid points to follow, the autonomy system switches to *Iceberg Reacquisition* mode. The vehicle first follows P_A , then follows an arc path around P_B .

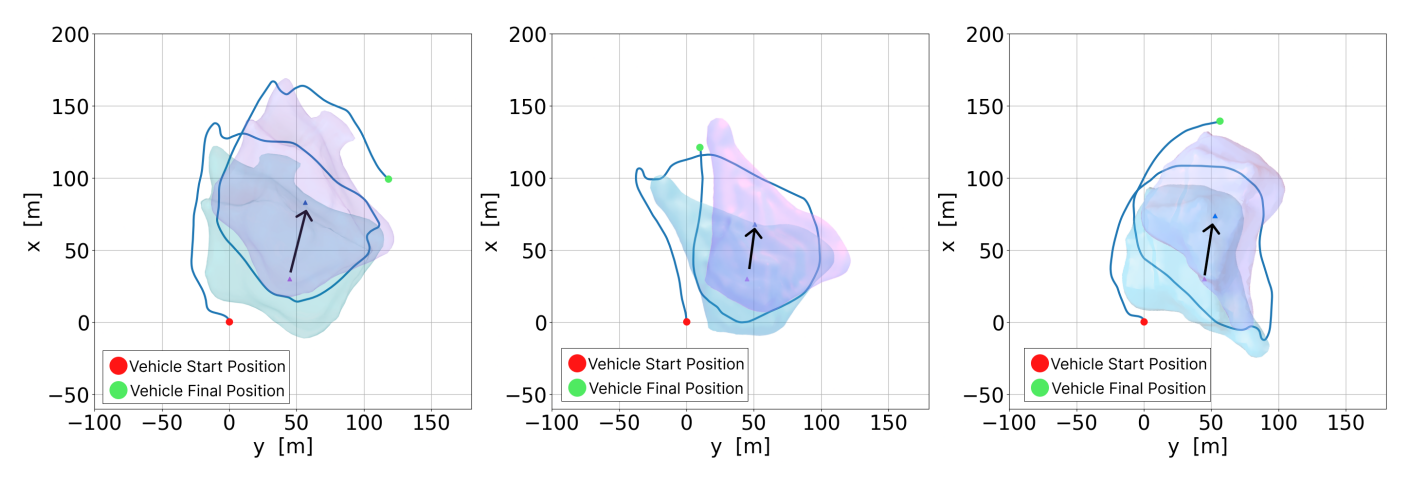


Fig. 8. The plot depicts the track of the vehicle while circumnavigating various iceberg shapes from the path derived from our algorithm.

2) Iceberg Reacquisition Mode: In the situation when the iceberg disappears from the FOV of the sonar, for example, at sharp corners or concave features, there will be no point for the vehicle to follow. In such cases, the autonomy system switches to *Iceberg Reacquisition Mode*. In this mode, the vehicle is instructed to follow a series of points based on its last seen point of the iceberg as shown in Figure 7. First, the vehicle is instructed to move towards PA that is determined by extending the last waypoint along the path by the standoff distance. Then, the autonomy system considers a point P_B which is laterally shifted towards starboard side of the vehicle by the stand-off distance from P_A. A sequence of points that form an arc ranging from 0 radian to $\pi/2$ radians are generated. These points are determined by the parametric equation of the circle. The vehicle is instructed to follow this arc after reaching P_A. Once the vehicle reacquires acoustic contact of the iceberg, enough to generate points, the autonomy system exits this behaviour and reverts back to Following mode.

III. VALIDATION

The method introduced in Section II is realized using ROS middleware and validated in the Stonefish simulator. We have integrated the proposed method on the simulated ALPHA AUV and tested on three different iceberg shapes from the database [15]. To better model the real situation, the iceberg is moving with a realistic speed (northward speed of 0.05 m/s, an eastward speed of 0.02 m/s and a rotational speed of 0.025 deg/s) from previous observations [16]. In the mission, the desired standoff distance is configured to 20 meters with a desired survey depth of 5 meters. The simulated MSIS returns are projected onto a local OGM using the costmap2d ROS package [17]. The waypoints are generated at 10Hz. Figure 8 presents the AUV tracks during circumnavigating on three iceberg shapes. To quantify the performance, we computed the distance from the AUV to the iceberg surface, as shown in Figure 9. The distance to the iceberg was calculated by measuring the distance of the closest y-coordinate in the OGM relative to the vehicle. The time periods where the vehicle was operated in Iceberg Reacquisition mode due to the lack of valid sonar points is highlighted in gray. Overall the root mean square error (RMSE) between the actual standoff distance and the desired value on the 3 icebergs was found to be 3.19m, 3.65m and 2.51m respectively. Discounting the *Iceberg Reacquisition* mode, the RMSE was found to be 2.9m, 2.9m and 2.3m respectively for the three icebergs. Improvement in lower RMS is observed compared to [18].

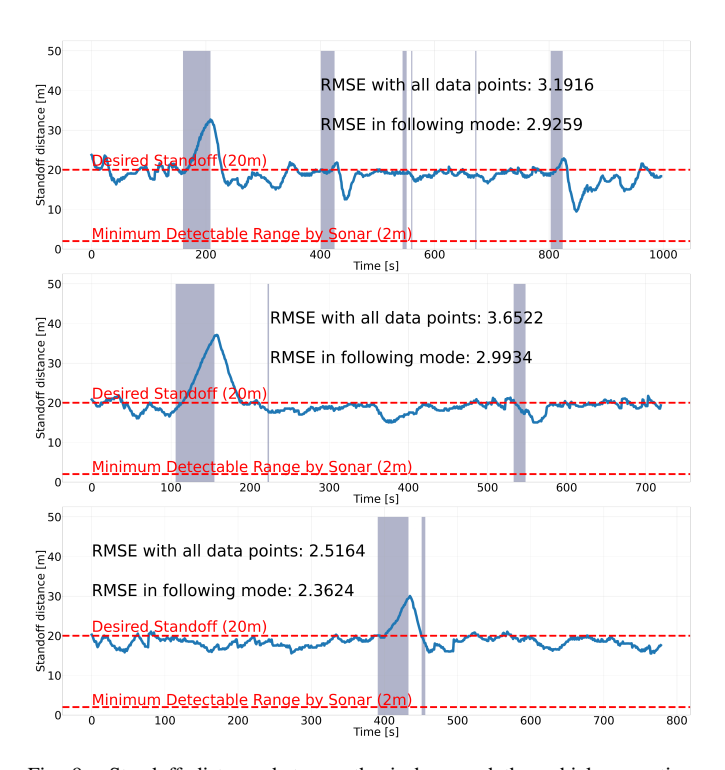


Fig. 9. Standoff distance between the iceberg and the vehicle over time compared to the desired standoff value. (Top: Figure 8 Left), (Middle: Figure 8 Middle), (Bottom: Figure 8 Right). The minimum detectable range of the SONAR is also noted (2 meters). The gray regions denote the times where there were no valid point present to follow. In such cases, autonomy system resorts to Iceberg Reacquisition Mode.

IV. CONCLUSION AND FUTURE WORKS

This paper presents a new autonomy system for AUV-based iceberg circumnavigation. Specifically, the paper introduces an algorithm to extract a guidance path based on an Occupancy Grid Map (OGM) constructed from the measurements from a Mechanical Scanning Imaging Sonar (MSIS). To better realize valid obstacle sonar returns, a new data processing pipeline and an adaptive filtering technique to construct occupancy grid maps is also presented. To utilize this path effectively, the paper introduces an algorithm that selects the waypoint to be followed by the AUV's guidance system. This autonomy system was tested and validated in a simulated environment with 3 different drifting icebergs. For future work, a mechanism to trigger completion of a circumnavigation loop needs to be implemented. This trigger can be used to alter the vehicle depth while on a iceberg mapping mission. The proposed method is planned to be tested with the ALPHA AUV in the field later this year. The pillars of Newport Pell Bridge are a potential candidate for the algorithms developed in this study. Circumnavigation around the base of one of the pillars would validate the effectiveness and robustness of the autonomy system.

REFERENCES

- [1] Y. Fang, "The impact of iceberg melting on the climate of the arctic circle," in *Proceedings of the 2022 6th International Seminar on Education, Management and Social Sciences (ISEMSS 2022)*. Atlantis Press, 2022, pp. 190–195.
- [2] R. S. McEwen, S. P. Rock, and B. Hobson, "Iceberg wall following and obstacle avoidance by an auv," in 2018 IEEE/OES Autonomous Underwater Vehicle Workshop (AUV), 2018, pp. 1–8.
- [3] P. W. Kimball and S. M. Rock, "Mapping of translating, rotating icebergs with an autonomous underwater vehicle," *IEEE Journal of Oceanic Engineering*, vol. 40, no. 1, pp. 196–208, 2015.
- [4] M. Zhou, R. Bachmayer, and B. Deyoung, "Mapping the underside of an iceberg with a modified underwater glider," *Journal of Field Robotics*, vol. 36, pp. 1037–1165, 04 2019.
- [5] P. Cieślak, "Stonefish: An advanced open-source simulation tool designed for marine robotics, with a ros interface," in OCEANS 2019 Marseille, 2019, pp. 1–6.
- [6] M. Zhou, E. C. Gezer, W. McConnell, and C. Yuan, "Acrobatic low-cost portable hybrid auv (alpha): System design and preliminary results," in OCEANS 2022, Hampton Roads, 2022, pp. 1–5.
- [7] A. Nunes, A. R. Gaspar, and A. Matos, "Occupancy grid mapping from 2d sonar data for underwater scenes," in OCEANS 2021: San Diego – Porto, 2021, pp. 1–8.
- [8] Grefstad and I. Schjølberg, "Navigation and collision avoidance of underwater vehicles using sonar data," in 2018 IEEE/OES Autonomous Underwater Vehicle Workshop (AUV), 2018, pp. 1–6.
- [9] J. Canny, "A computational approach to edge detection," *IEEE Transactions on Pattern Analysis and Machine Intelligence*, vol. PAMI-8, no. 6, pp. 679–698, 1986.
- [10] P. Norgren-Aamot and R. Skjetne, "Line-of-sight iceberg edge-following using an auv equipped with multibeam sonar," *IFAC-PapersOnLine*, vol. 48, pp. 81–88, 12 2015.
- [11] S. Weisberg, "Applied linear regression," F. Balding, Cressie, Ed. Wiley, 2014, ch. 2.
- [12] Y. Noguchi, Y. Sekimori, and T. Maki, "Guidance method of underwater vehicle for rugged seafloor observation in close proximity," *Journal of Field Robotics*, vol. 41, 11 2023.
- [13] M. Breivik and T. Fossen, Guidance Laws for Autonomous Underwater Vehicles, 01 2009.
- [14] E. C. Gezer, M. Zhou, L. Zhao, and W. McConnell, "Working toward the development of a generic marine vehicle framework: Ros-mvp," in OCEANS 2022, Hampton Roads, 2022, pp. 1–5.

- [15] T. G. Barker A, Skabova I, "Iceberg visualizataion database." National Research Council Canada, Canadian Hydraulics Centre, Tech. Rep., 1999
- [16] M. Zhou, R. Bachmayer, and B. de Young, "Surveying a floating iceberg with the usv seadragon," in *Frontiers in Marine Science*, 2021. [Online]. Available: https://api.semanticscholar.org/CorpusID:235813152
- [17] D. V. Lu, D. Hershberger, and W. D. Smart, "Layered costmaps for context-sensitive navigation," in 2014 IEEE/RSJ International Conference on Intelligent Robots and Systems, 2014, pp. 709–715.
- [18] M. Zhou, R. Bachmayer, and B. Deyoung, "Towards autonomous underwater iceberg profiling using a mechanical scanning sonar on a underwater slocum glider," 11 2016.